ELSEVIER

Synthesis and in vitro properties of trimethylamine- and phosphonate-substituted carboranylporphyrins for application in BNCT

Michael W. Easson, Frank R. Fronczek,* Timothy J. Jensen and M. Graça H. Vicente*

Department of Chemistry, Louisiana State University, Baton Rouge, LA 70803-1804, USA

Abstract—A series of carboranylporphyrins containing either amine or phosphonic acid functionalities and two to six *closo*-carborane clusters have been synthesized via a [2 + 2] condensation of a dimethylamino- or diethylphosphonate-substituted dipyrromethane with a dicarboranylmethyl-benzaldehyde. The X-ray structures of four key reaction intermediates (**1**, **2**, **3**, and **4a**) and of two target porphyrins, the diphosphonate ester- and the diamino-tetracarboranylporphyrins **5b** and **6a**, are presented and discussed. In vitro studies using human carcinoma HEp2 and human glioblastoma T98G cells show that these porphyrins are non-toxic in the dark up to 100 μM concentrations, and that a tetracarboranylporphyrin bearing two quaternary ammonium groups is the most efficiently taken up by cells at short times (up to 8 h), followed by a dicarboranylporphyrin bearing three phosphonic acid substituents. All carboranylporphyrins delivered therapeutic amounts of boron to T98G cells and localized mainly within the cell lysosomes.
© 2007 Elsevier Ltd. All rights reserved.

1. Introduction

Boron neutron capture therapy (BNCT) is a binary therapy that involves the activation of a tumor-localized ^{10}B-containing sensitizer with low energy neutrons, resulting in the release of high linear energy transfer (high-LET) particles (^{4}He^{2+} and ^{7}Li^{3+}) containing 2.4 MeV of kinetic energy.[1–3] The short-range high-LET particles are highly cytotoxic and thus can selectively destroy ^{10}B-containing malignant cells in the presence of boron-free normal tissues. BNCT is particularly attractive for the treatment of high-grade gliomas, malignant melanomas, meningiomas, head and neck tumors, and oral cancer.[4] Two boron-containing compounds, mercapto-*closo*-dodecaborate (BSH) and 4-dihydroxyborylphenylalanine (BPA), are currently being used in BNCT clinical trials, in the USA, Europe, and Japan.[4–9] Since in the clinical studies performed to date there has been evidence of a therapeutic response to BNCT, the discovery of BNCT agents with higher biological efficacy than BSH and BPA has been an active area of research. Several boron-containing molecules have been synthesized and investigated as boron delivery agents for BNCT, including nucleosides, amino acids, phospholipids, monoclonal antibodies, dendrimers, and porphyrins.[10,11] Among these, porphyrins are very promising boron delivery vehicles because of their known tumor selectivity, low dark toxicity, and long persistence within tumors.[12,13] A promising BNCT delivery porphyrin agent should exhibit the following characteristics: (1) low dark toxicity, (2) high tumor cell selectivity, that is, high tumor/normal tissue and tumor/blood boron concentration ratios, (3) deliver therapeutic concentrations of ^{10}B to tumors, that is, >20 μg ^{10}B/g tumor,[4] (4) localize within tumor cells, preferentially within or near sensitive organelles such as the nuclei,[14,15] (5) have long retention times within tumors and rapid clearance from normal tissues and blood, and (6) be easily monitored by fluorescence techniques in order to facilitate radiation dosimetry. The major challenge in the development of BNCT delivery agents has been the selective delivery of therapeutic amounts of boron to targeted tumors with minimal normal tissue toxicity.[4]

Herein we report the syntheses of new amphiphilic *closo*-carboranylporphyrins (**5d**, **6c,d**, **7c,d**, and **8d**) bearing either positively charged quaternary ammonium or negatively charged phosphonate water-solubilizing groups,

and two to six *closo*-carborane cages.[16] Only a few water-soluble *closo*-carboranylporphyrins have been previously reported in the literature, bearing carboxylates or a PEG as water-solubilizing groups.[12] Our new *closo*-carboranylporphyrins contain either phosphonate groups that can form multiple hydrogen bonds with biological molecules, or quaternary ammonium salts that can potentially target highly vulnerable intracellular sites, such as the nuclei, and induce effective DNA and RNA damage.[17–20] The X-ray molecular structures of four key intermediates (**1**, **2**, **3**, and **4a**) and of two target porphyrins (**5b** and **6c**) are discussed. We investigated and compared the in vitro toxicity, cellular uptake, and subcellular distribution properties of this series of

compounds using both human carcinoma HEp2 and human glioblastoma T98G cells.

2. Results

2.1. Porphyrin syntheses

Porphyrins **5**–**8** containing two to six carborane cages (18–38% boron by weight) were synthesized via a [2 + 2] condensation of dicarboranyl-benzaldehyde **3** with an amine- or phosphonate-substituted dipyrromethane **4**, as shown in Scheme 1. Due to acid-catalyzed scrambling in these reactions porphyrins **5**–**8** were ob-
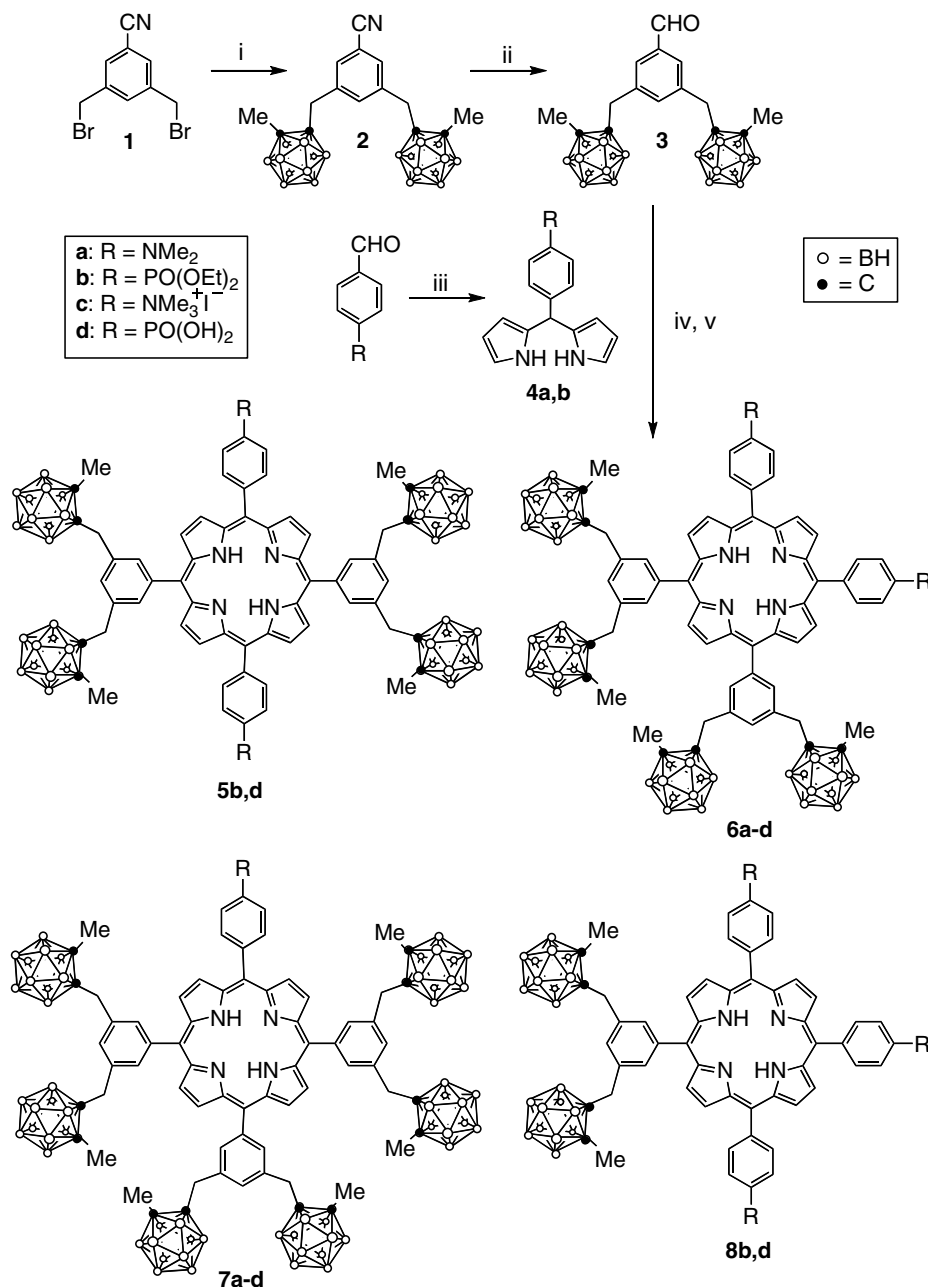
Scheme 1. Reagents and conditions: (i) 1-Lithium-2-methyl-*o*-carborane, THF, LiI, rt, 20 h (51%); (ii) DIBAL, toluene followed by 10% H$_2$SO$_4$ (62%); (iii) pyrrole, TFA, CH$_2$Cl$_2$, rt (70–86%); (iv) BF$_3$OEt$_2$, CH$_2$Cl$_2$, rt, 4 min–1 h; (v) DDQ, rt for 30 min (overall 17–22%).

tained in a single-pot reaction and isolated in 2–8% yields, along with 2–9% of the corresponding octa-carboranylporphyrin (H$_2$OCP),[21] and <1% of other minor porphyrin products. The benzonitrile **1**, prepared according to the procedure of Bodwell et al.,[22] reacted with in situ prepared 1-lithium-2-methyl-*o*-carborane producing the dicarboranyl-benzonitrile **2** in 51% yield. The cyano group of compound **2** was reduced to formyl using DIBAL-H, giving benzaldehyde **3** in 62% yield. We have previously reported a related synthesis of dicarboranyl-benzaldehyde **3**[23] from 3,5-dimethyl-bromobenzene in 15% overall yield. Our new synthesis of **3** relies on the readily reduction of the cyano group of **2**, as previously reported for other benzonitriles,[24] rather than on a lithium/bromide exchange followed by DMF addition and acidic hydrolysis,[23] thus involving less steps. Dipyrromethanes **4** were prepared from the reaction of the corresponding benzaldehyde with an excess of pyrrole using TFA as the catalyst, in 70–86% yields, as previously reported.[25–27] The condensation of compounds **3** and **4a** via a [2 + 2] methodology,[27–29] using BF$_3$OEt$_2$ for 1 h at room temperature, followed by oxidation with 2,3-dichloro-5,6-dicyano-1,4-benzoquinone (DDQ) gave porphyrins **6a**, **7a** and H$_2$OCP in 2.1%, 6.3% and 8.5% yields, respectively, as major products. On the other hand, the condensation of **3** and **4b** under similar conditions but using BF$_3$OEt$_2$ for only 4 min afforded porphyrins **5b**, **6b**, **7b**, **8b** and H$_2$OCP in 3.6%, 2.6%, 8.0%, 4.5% and 2.1% yields, respectively. Other porphyrins were also obtained as minor products (<1% yield) as a result of the scrambling but were not isolated in sufficient amounts for characterization. In order to achieve water-solubility, the phosphonate esters were cleaved to the corresponding phosphonic acids using bromotrimethylsilane followed by hydrolysis[30] in 78–99% yields, and the dimethylamino groups were quaternized with excess iodomethane,[19] in 83–92% yields. While the porphyrins containing either the diester phosphonate or dimethylamino functionalities are highly soluble in dichloromethane, the phosphonic acid-containing porphyrins are only soluble in DMSO and partially soluble in water, and the trimethylammonium-porphyrins are soluble in polar solvents (such as acetone and methanol) and also partially water-soluble. Porphyrin **5d** exhibited particularly low solubility in all solvents, including DMSO, and therefore was not evaluated in in vitro studies.

2.2. Molecular structures

Crystals of intermediate dibromobenzonitrile **1** were grown from ethyl acetate/hexane, and those of carboranyl-benzonitrile **2**, carboranyl-benzaldehyde **3**, and dipyrromethane **4a** were grown from CHCl$_3$/hexane. Their molecular structures are shown in Figures 1–4, respectively, confirming their identities. Crystals of the toluene solvate of porphyrin **5b** were grown from CHCl$_3$/toluene, and those of the chloroform solvate of **6a** were obtained by slow evaporation of a chloroform solution over a period of several days. The X-ray structures of porphyrins **5b** and **6a** are shown in Figures 5 and 6, respectively. In the crystal, porphyrin **5b** lies on an inversion center, so the four N atoms are symme-
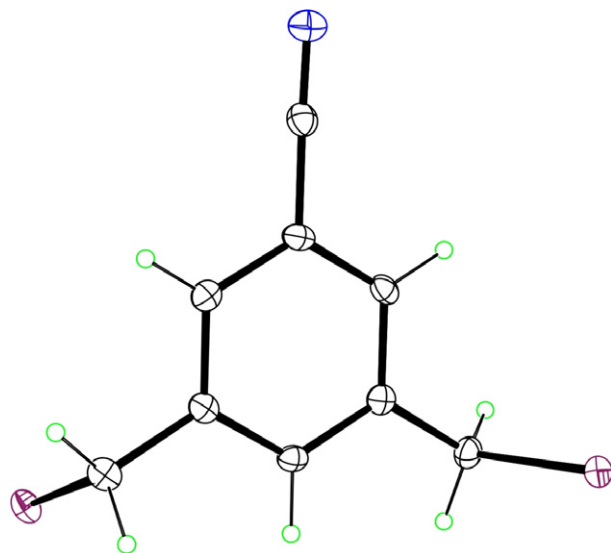

Figure 1. The molecular structure of **1** as determined by X-ray crystallography, with ellipsoids at the 50% level.

try-required to be rigorously coplanar. The entire porphyrin ring deviates little from coplanarity, exhibiting a mean deviation of 0.029 Å for the 24-atom core and maximum deviation of 0.067(4) Å. The phenyl rings carrying the phosphonates form dihedral angles of 70.9(1)° with the porphyrin plane, and the phenyl rings carrying the carboranes form dihedral angles of 67.0(1)° with it. In porphyrin **6a**, the four porphyrin N atoms in Figure 6 are coplanar within 0.02(2) Å, but the 24-atom porphyrin core deviates somewhat from planarity, its atoms exhibiting a mean deviation of 0.12 Å from their best plane, with maximum deviation of 0.26(3) Å. The distortion is mostly a twist about an axis bisecting the pyrrole between the two Me$_2$NPh groups and the pyrrole between the two carborane-substituted phenyl groups. This twist places the two NMe$_2$ nitrogen atoms 1.54(4) and −0.70(3) Å above and below the porphyrin best plane, as illustrated in Figure 6a, a view down the twist axis. The phenyl rings form dihedral angles which fall in the range 71.3(6)–82.3(6)° with the porphyrin best plane.

2.3. Dark cytotoxicity

The dark toxicity of porphyrins **6c**, **6d**, **7c**, **7d**, and **8d** toward human carcinoma HEp2 cells was evaluated at concentrations up to 100 μM and the results obtained are shown in the Supplementary data. All compounds were found to be non-toxic to HEp2 cells in the dark under the conditions tested, up to 100 μM concentrations.

2.4. Cellular uptake

The time-dependent uptake of porphyrins **6c**, **6d**, **7c**, **7d**, and **8d** was evaluated in human glioblastoma T98G cells at a concentration of 10 μM over a period of 24 h and the results are shown in Figure 8. All porphyrins accumulated rapidly in the first 2 h, after which a plateau was reached for **6c**, **6d**, **7c**, and **7d**, while **8d** continued to steadily accumulate over time up to the 24 h period investigated. Porphyrin **6c** bearing two quaternary
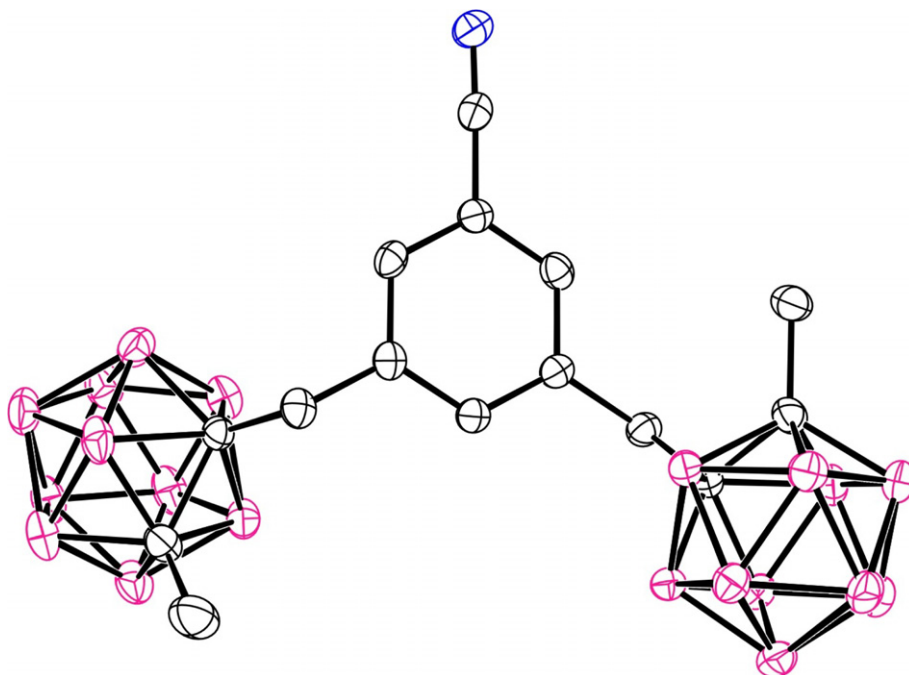
Figure 2. The molecular structure of **2** with 50% ellipsoids. H atoms are not shown.
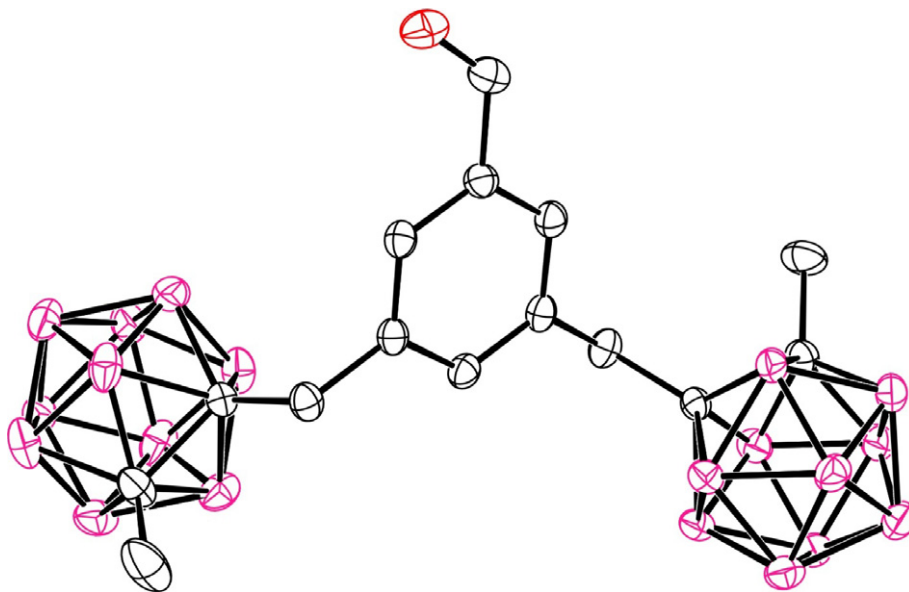

Figure 3. The molecular structure of **3** with 50% ellipsoids. H atoms are not shown.

ammonium groups on adjacent *p*-phenyl positions accumulated the most of this series of compounds at short time points (<4 h), while porphyrin **8d** with three phosphonic acid groups accumulated the most at longer time points (>8 h). Porphyrin **7c** containing only one quaternary ammonium group was the least taken-up by the T98G cells at all time points investigated. Similar uptake results were also obtained using human carcinoma HEp2 cells (results not shown).

2.5. Intracellular localization

Fluorescence microscopy was used to investigate the preferential sites of intracellular localization of porphy-

rins **6c**, **6d**, **7c**, **7d**, and **8d**, using both HEp2 and T98G cells. The cells were exposed overnight to 10 μM of each porphyrin and then examined for intracellular fluorescence. Similar results were obtained with both cell lines; Figures 9b–13b show the fluorescence patterns observed in HEp2 cells. For the co-localization experiments the cells were incubated concurrently with porphyrin and one of the following organelle tracers for 30 min: Mito-Tracker Green 250 nM, LysoSensor Green 50 nM, BODIPY FL C_5-ceramide at 1 mM and ER Tracker Green FM 2 μg/mL. The slides were washed three times with growth medium and new medium containing 50 mM HEPES, pH 7.4, was added. The images were acquired using a Zeiss Axiovert 200 M inverted fluores-
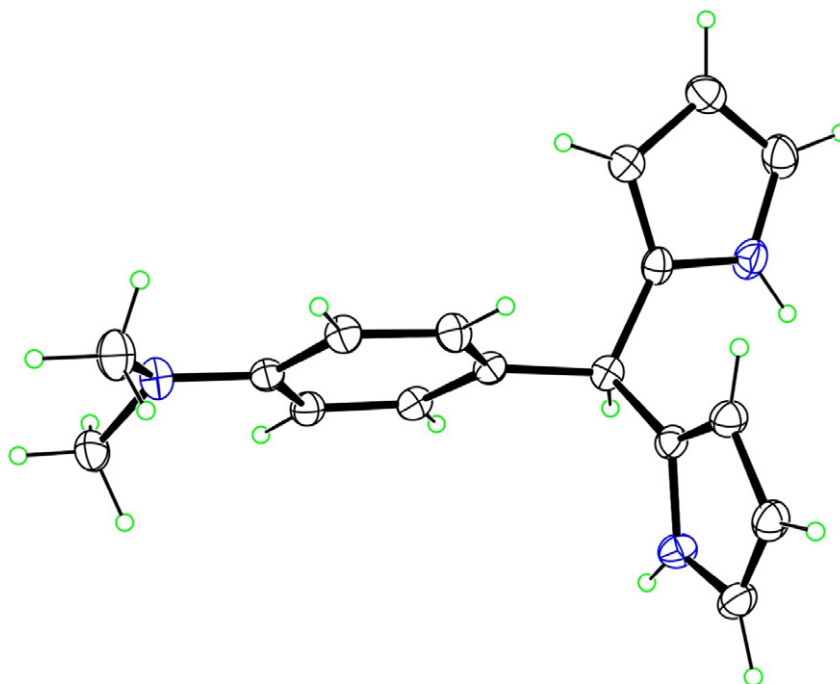
Figure 4. The molecular structure of **4a** with 50% ellipsoids.

cence microscope fitted with standard FITC and Texas Red filter sets. The preferential site of intracellular localization for porphyrins **6c**, **6d**, **7c**, **7d**, and **8d** was found to be the lysosomes (Figs. 9f–13f).

3. Discussion

The new series of *closo*-carboranylporphyrins **5–8** was prepared in a single reaction using a MacDonald-type [2 + 2] condensation[31] of either dimethylamino- or diethylphosphonate–dipyrromethane with dicarboranyl-benzaldehyde **3** (Scheme 1). We investigated various reaction conditions that led to the highest yields of the target porphyrins **5–8**, bearing one to three water-solubilizing groups and two to six *closo*-carborane cages, including different acid catalysts, reagent concentrations, solvents, reaction times, and temperatures.[27,28] The optimal conditions involved the use of 10 mM dipyrromethane and benzaldehyde concentrations in dichloromethane and 2 equiv of BF_3OEt_2 for either 1 h (in the case of **4a** + **3**) or 4 min (for **4b** + **3**). The use of dipyrromethanes **4** in a [2 + 2] condensation rather than a mixed aldehyde condensation afforded higher yields of the target porphyrins containing at least one dipyrromethane motif, by minimizing the formation of H_2OCP, which was always a side product in these reactions. When 5-(4-acetamidophenyl)dipyrromethane was used in place of **4a**, lower yields of the targeted porphyrins were obtained due to the additional step required to cleave the acetamido group (ethanol/HCl at reflux for 24 h) and the isolation of a tetracarboranylcorrole as one of the main products. The condensation of 5-[bis(3,5-(2-methyl-*o*-carboran-1-yl)methyl)phenyl]dipyrromethane with phosphonate- or amino-substituted benzaldehydes also gave lower yields of the targeted

porphyrins;[16] in fact, no carborane-containing phosphonate-substituted porphyrins were obtained using this methodology. The acid-catalyzed scrambling was more significant in the [2 + 2] condensation of **4a** with **3** probably as a result of the strong electron-donating effect of the dimethylamino group and the longer reaction time necessary to drive the reaction to completion; in this case the *trans*-porphyrin **5a** was not among the major products of the reaction and H_2OCP was the main product obtained in 8.5% yield. Under the above optimal conditions for the condensation of **4b** and **3**, porphyrin **7b** bearing a single phosphonate ester was the major product obtained, followed by **8b** and **6b**; in this case H_2OCP was only obtained in 2.1% yield. Although acid-catalyzed scrambling reactions are generally avoided in order to minimize challenging chromatographic separations, this methodology allowed us to isolate reasonable amounts of several interesting porphyrin targets for structure/in vitro biological activity relationships.

All new compounds were characterized by spectroscopic techniques (MS, ^{1}H NMR, UV–Vis) and in addition, benzonitriles **1** and **2**, benzaldehyde **3**, dipyrromethane **4a**, and porphyrins **5b** and **6a** were also characterized by X-ray crystallography. It is interesting to note that while the porphyrin ring in porphyrin **5b**, bearing two phosphonic esters on opposite *p*-phenyl positions is essentially flat, that of porphyrin **6a** with two adjacent *p*-dimethylaminophenyl groups is moderately distorted from planarity, showing a twisted conformation. Such porphyrin distortions from planarity have been previously observed[32] and seem to be associated with the electronic interactions between the water-solubilizing groups rather than with the 3,5-dicarboranylmethylphenyl groups.[21,23] Upon quaternization of the dimethyl-
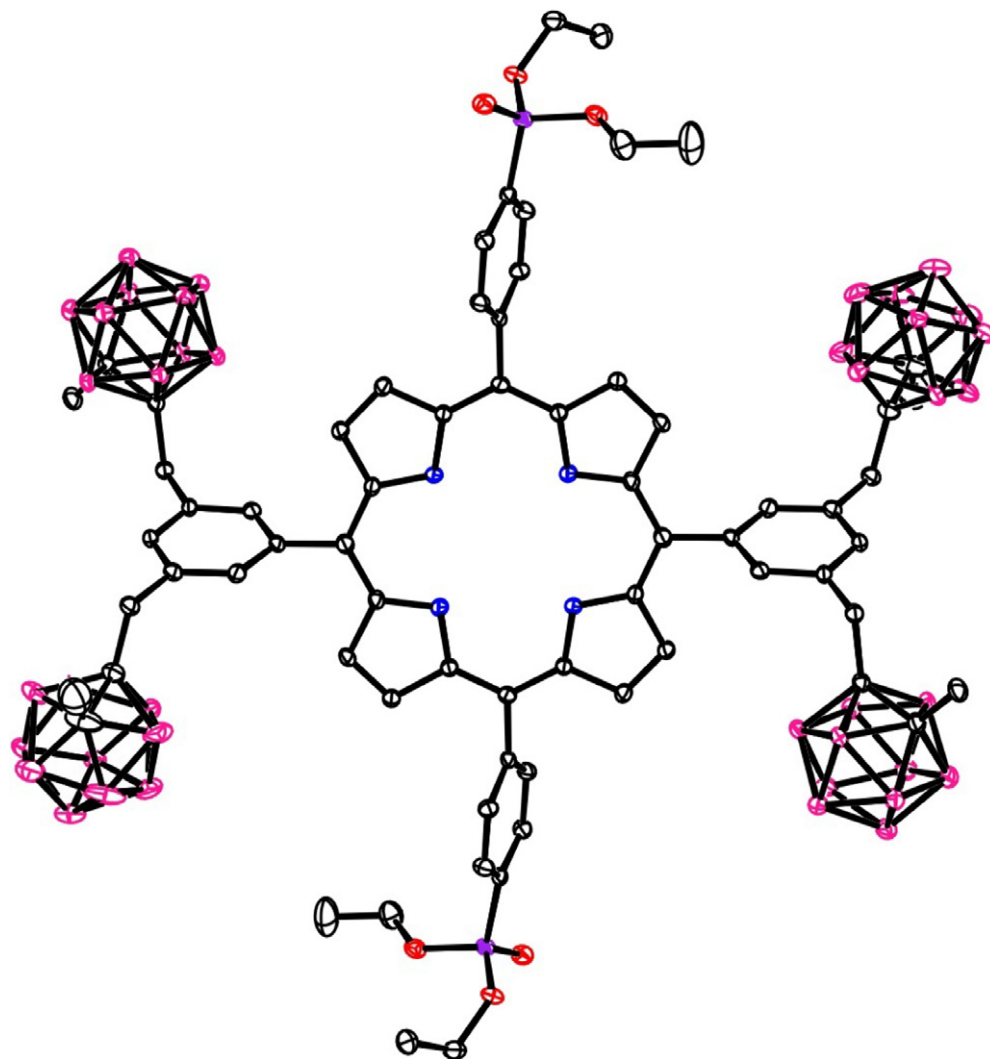
Figure 5. The molecular structure of porphyrin **5b** with 20% ellipsoids. Solvent molecules and H atoms are not shown.

amino groups of **6a**, that is, in **6c**, a more pronounced distortion of the porphyrin is expected, as we have previously observed for a 5,10-di(4-trimethylamino)phenyl-15,20-diphenylporphyrin.[19]

As a consequence of the highly hydrophobic character of the *closo*-carborane cages, porphyrins **5b**, **6a,b**, **7a,b**, and **8b** were completely insoluble in water. Two strategies are usually employed for conferring partial water-solubility to carboranylporphyrins,[12] (1) the introduction of water-solubilizing groups (such as amino, hydroxyl or carboxylate), or (2) the deboronation of *o*-carborane cages to the corresponding anionic *nido*-carboranes. In the present study we synthesized, characterized, and compared the in vitro biological properties of a new series of *closo*-carboranylporphyrins bearing either positively charged quaternary ammonium or negatively charged phosphonate water-solubilizing groups; these compounds could potentially interact with DNA[33,34] and the phosphonate-substituted porphyrins could form multiple hydrogen bonds with biological substrates. Interestingly, porphyrin **5d** bearing two phosphonic acid substituents on opposite *p*-phenyl positions showed very limited water-solubility, probably as a

result of the formation of large aggregates and their subsequent precipitation in aqueous media.[35] Porphyrins **5d**, **6c**, **6d**, **7c**, **7d**, and **8d** showed similar absorption and emission spectra in DMSO, typical for *meso*-tetraphenylporphyrins, as shown in Figure 7. However, in HEPES buffer (20 mM, pH 7.4) containing 1% DMSO all porphyrins showed significant broadening of their emission bands and fluorescence quenching indicating aggregation (see Fig. 7 and Supplementary data), as we have previously observed.[36] Interestingly, porphyrins **5d**, **6c**, **7c**, and **7d** displayed red-shifted (1–4 nm) emission bands, while porphyrins **6d** and **8d** showed blue-shifted (3–5 nm) bands, suggesting the formation of different types of aggregates.

Porphyrins **6c**, **6d**, **7c**, **7d**, and **8d** were all found to be non-toxic to HEp2 cells in the dark up to 100 μM concentrations (see Supplementary data). Higher concentrations were not investigated because the compounds precipitated. Our results are in agreement with previous studies reporting very low dark toxicities for both *closo*- and *nido*-carboranylporphyrins.[21,23,34,36–42] The cellular uptake of this series of *closo*-carboranylporphyrins did not increase with their hydrophobic character. We deter-
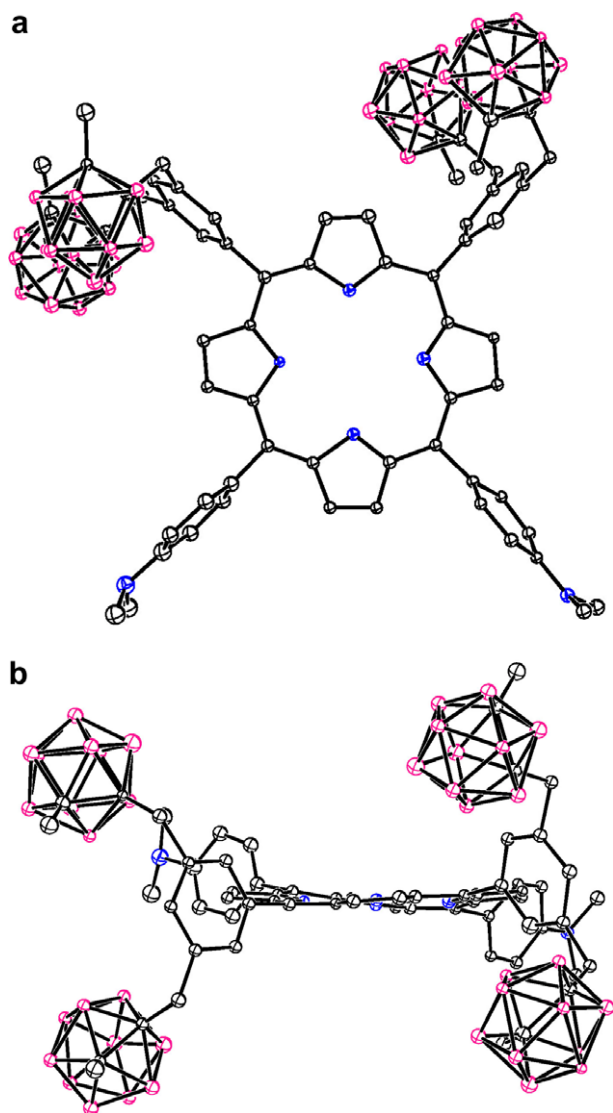
Figure 6. The molecular structure of porphyrin **6a** with 20% spheres. (a) top view; (b) side view. Solvent molecules and H atoms are not shown.

mined the following order of increasing uptake at times <8 h: **6c** > **8d** > **7d** > **6d** > **7c** (Fig. 8). At longer time periods porphyrin **8d**, bearing three phosphonic acid groups, was the most accumulated within cells, and at 24 h twice the amount of this porphyrin was found within cells than **6d**, containing two phosphonic acid groups on adjacent phenyl rings. Porphyrin **7d** with only one phosphonic acid substituent and the highest percentage of boron by weight of all porphyrins showed slightly higher uptake than **6d** at all time points investigated and delivered the highest amount of boron to T98G cells after 24 h (see Table 1 in Supplementary data). After 24 h the calculated amount of intracellular boron (in µg per billion cells or per gram of wet tissue) delivered by the porphyrins to T98G cells was between 92.6 ± 16.2 (for **7c**) and 220.0 ± 35.0 (for **7d**). Therefore, all porphyrins are able to deliver therapeutic amounts of boron to human glioblastoma T98G cells. The differences in uptake observed for the phosphonate-containing porphyrins might be due to the unique aggregation

behavior of these polyprotic compounds, as we have previously investigated.[35] At physiologic pH the phosphonic acid groups mainly exist in their mono-anionic form (i.e., as PO_3H^-) and the resulting anionic porphyrins can aggregate as a result of both π-π interactions and hydrogen bond formation. It has been recently shown that negatively charged cobaltacarborane-porphyrins containing up to eight negative charges form large aggregates in aqueous solutions.[36,43] On the other hand, porphyrin **6c**, bearing two quaternary ammonium groups, accumulated within T98G cells about 2.5 times more than **7c** with only one positive charge; in fact porphyrin **7c** was the least taken up by cells of all the porphyrins studied and delivered the least amount of boron to T98G cells. The higher amphiphilicity of porphyrin **6c** compared with **7c** as a result of its more favorable lipophilic/hydrophilic balance as a consequence of its charge distribution might be responsible for the observed results. The uptake kinetics for this series of carboranylporphyrins is similar to that previously observed for both *closo*- and *nido*-carboranylporphyrins.[21,36,37,39,44,45]

The preferential sites of intracellular localization for porphyrins **6c**, **6d**, **7c**, **7d**, and **8d** were found to be the cell lysosomes, as evidenced by the punctate pattern observed by fluorescence microscopy and its overlay with the lysosome-specific probe LysoSensor Green. These results are in agreement with previous studies showing that carboranylporphyrins localize within cell lysosomes,[21,36,39,45–48] maybe as a result of an endocytic mechanism of uptake.[49,50]

4. Conclusions

The syntheses of six new amphiphilic *closo*-carboranylporphyrins bearing either positively charged quaternary ammonium (**6c**,**7c**) or negatively charged phosphonate (**5d**, **6d**, **7d**, and **8d**) groups are reported. The X-ray molecular structures of four intermediates (**1**, **2**, **3**, and **4a**) and of two target porphyrins (**5b** and **6c**) are discussed. All porphyrins were found to be non-toxic in the dark up to 100 µM concentrations and the extent of their cellular uptake did not increase with their hydrophobic character. The tetracarboranylporphyrin **6c**, bearing two quaternary ammonium groups, was the most efficiently taken up by human glioma T98G cells at short times (up to 8 h), followed by dicarboranylporphyrin **8d** bearing three phosphonic acid substituents. The hexacarboranylporphyrin **7d** was found to deliver the highest amount of boron to T98G cells after 24 h. The preferential sites of subcellular localization of this series of porphyrins were found to be the cell lysosomes.

5. Experimental

5.1. Chemistry

All reactions were carried out under an argon atmosphere in dried solvents. Commercially available starting compounds were purchased from Sigma-Aldrich or
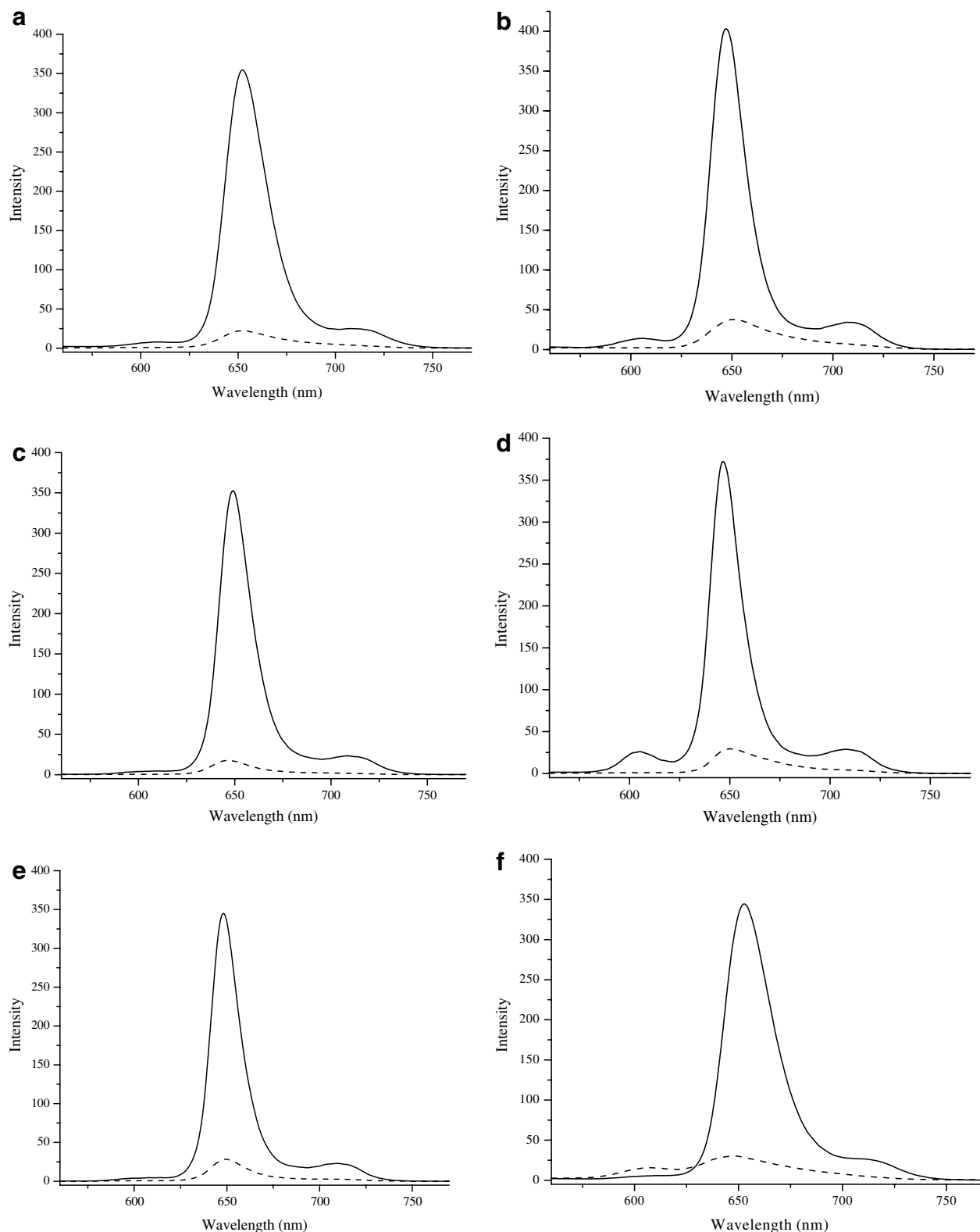
Figure 7. Fluorescence emission spectra of porphyrins **5d** (a), **6c** (b), **6d** (c), **7c** (d), **7d** (e), and **8d** (f), at 1×10^{-6} M in DMSO (solid line), and in freshly prepared HEPES buffer (20 mM, pH 7.4) containing 1% DMSO (dashed line). Excitation at 420 nm.

from Katchem, Ltd. and used directly without further purification. Silica gel 60 (70–230 mesh, Merck) was used for column chromatography. Analytical thin-layer chromatography (TLC) was performed using Merck 60 F254 silica gel (precoated sheets, 0.2 mm thick). [1]H

NMR spectra were obtained using a Bruker DPX 250 MHz spectrometer; chemical shifts are expressed in ppm relative to TMS (0 ppm). Electronic absorption spectra were measured on a Perkin Elmer Lambda 35 UV–Vis spectrophotometer. Low resolution mass spec-
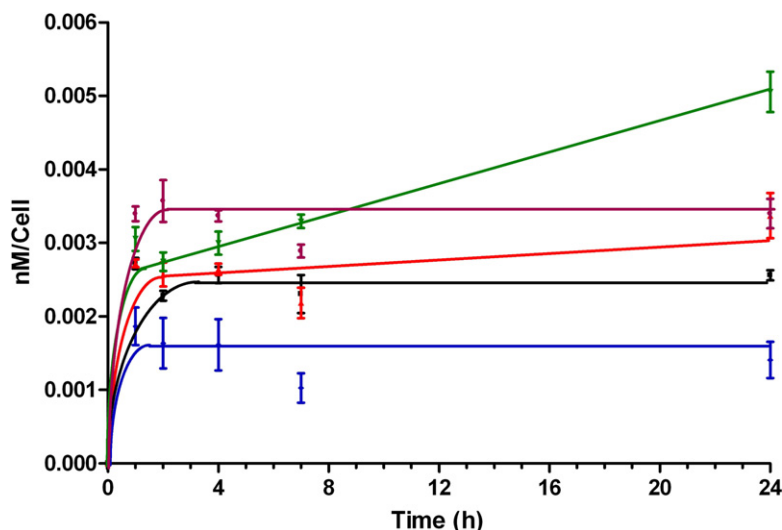
Figure 8. Time-dependent uptake of porphyrins **6c** (purple), **6d** (black), **7c** (blue), **7d** (red), and **8d** (green) at 10 μM by T98G cells.

tra (MS) were obtained on a Bruker Proflex III MAL-DI-TOF mass spectrometer. High resolution mass spectra (HRMS) were obtained using ESI-TOF under negative mode on an Agilent Technologies Time-of-Flight LC/MS 6210; the isotope peaks were matched with calculated isotope patterns (see Supplementary data) and only the most abundant peaks are listed below for each porphyrin. Melting points were measured on a MELT-TEMP apparatus.

5.1.1. Bis(3,5-bromomethyl)benzonitrile (1).[22] To a round-bottomed flask containing dichloromethane (460 mL) were added 3,5-dimethylbenzonitrile (5.00 g, 38 mmol), NBS (15.00 g, 84 mmol), and benzoyl peroxide (0.048 g, 0.20 mmol). The reaction mixture was heated to reflux while stirring under argon. Upon reaching reflux a white floodlight was positioned within four inches of the reaction vessel. After 1 h the reaction mixture was cooled to room temperature and 50 mL of distilled water was added to quench the reaction. The organic phase was washed once with water, once with brine, and then dried over Na_2SO_4, and the solvent removed under vacuum to yield a yellow/orange residue. The crude residue was dried onto silica and purified by silica gel column chromatography using ethyl acetate/hexane 1:4 for elution. The pure product was collected affording 4.47 g of the title compound as a white solid in 40% yield. Mp = 114–115 °C; MS (GC) m/z 289.8 [M+1]; ^1H NMR (CDCl$_3$) δ ppm: 4.50 (s, 4H, CH$_2$), 7.65 (s, 2H, o-ArH), 7.68 (s, 1H, p-ArH).

5.1.2. Bis[3,5-(2-methyl-o-carboran-1-yl)methyl]benzonitrile (2). n-Butyllithium (23.63 mL, 1.6 M in hexane) was added dropwise to a solution of 1-methyl-o-carborane (4.76 g, 30 mmol) in dry THF (450 mL) at a temperature between −5 and 0 °C, under argon. The mixture was stirred at this temperature for 1.5 h, and then compound **1** (4.37 g, 15.10 mmol) and LiI (0.628 g, 4.69 mmol) in THF (50 mL) were added. The final reaction mixture was allowed to warm to room temperature and after 20 h the reaction was quenched with water and the solvent removed under vacuum.

The crude residue was dissolved in ethyl acetate and washed once with water, once with brine, dried over Na_2SO_4, and the solvent removed under vacuum. The yellow residue was dried onto silica and purified by silica gel column chromatography using ethyl acetate/hexane 1:4 for elution. The pure title compound was obtained as an off-white solid (2.70 g) in 51% yield (40% conversion). Recovered 1.05 g of compound **1**. Mp = 235–237 °C; MS (ESI) m/z 443.24; ^1H NMR (CDCl$_3$) δ ppm 1.4–3.0 (br s, 20H, BH), 2.22 (s, 6H, CH$_3$), 3.58 (s, 4H, CH$_2$), 7.36 (s, 1H, p-ArH), 7.56 (s, 2H, o-ArH).

5.1.3. Bis[3,5-(2-methyl-o-carboran-1-yl)methyl]benzaldehyde (3). A solution of compound **2** (11.14 g, 25.14 mmol) in dry toluene (500 mL) was flushed with argon for 10 min. The reaction vessel was then cooled to 0 °C and DIBAL-H (1.5 M in toluene) (36.87 mL, 55.3 mmol) was slowly added dropwise while stirring under argon. The reaction was heated to 60–65 °C for 39 h, then cooled to 0 °C and a cold 10% H_2SO_4 aqueous solution (228 mL) was slowly added to avoid foaming. Toluene (800 mL) was added and the reaction mixture was stirred for an additional 62 h under argon. The organic phase was washed once with Na_2HCO_3, once with water, once with brine, dried over Na_2SO_4, and the solvent removed under vacuum to yield a crude white solid. This solid was dissolved in dichloromethane, dried onto silica, and purified by silica gel column chromatography using 1:1 hexane/dichloromethane for elution. Pure title compound was obtained as a white solid (7.07 g) in 62% yield. The spectroscopic data for the title compound are in full agreement with those reported in the literature.[21,23]

5.1.4. 5-(4-Dimethylamino)phenyldipyrromethane (4a). The title compound was prepared as described in the literature and its spectroscopic data are in full agreement with those previously reported.[27]

5.1.5. 5-(4-Phosphonate diethylester)phenyldipyrromethane (4b). A solution of 4-(phosphonate diethyl ester) benzaldehyde (0.047 g, 0.20 mmol) and freshly distilled
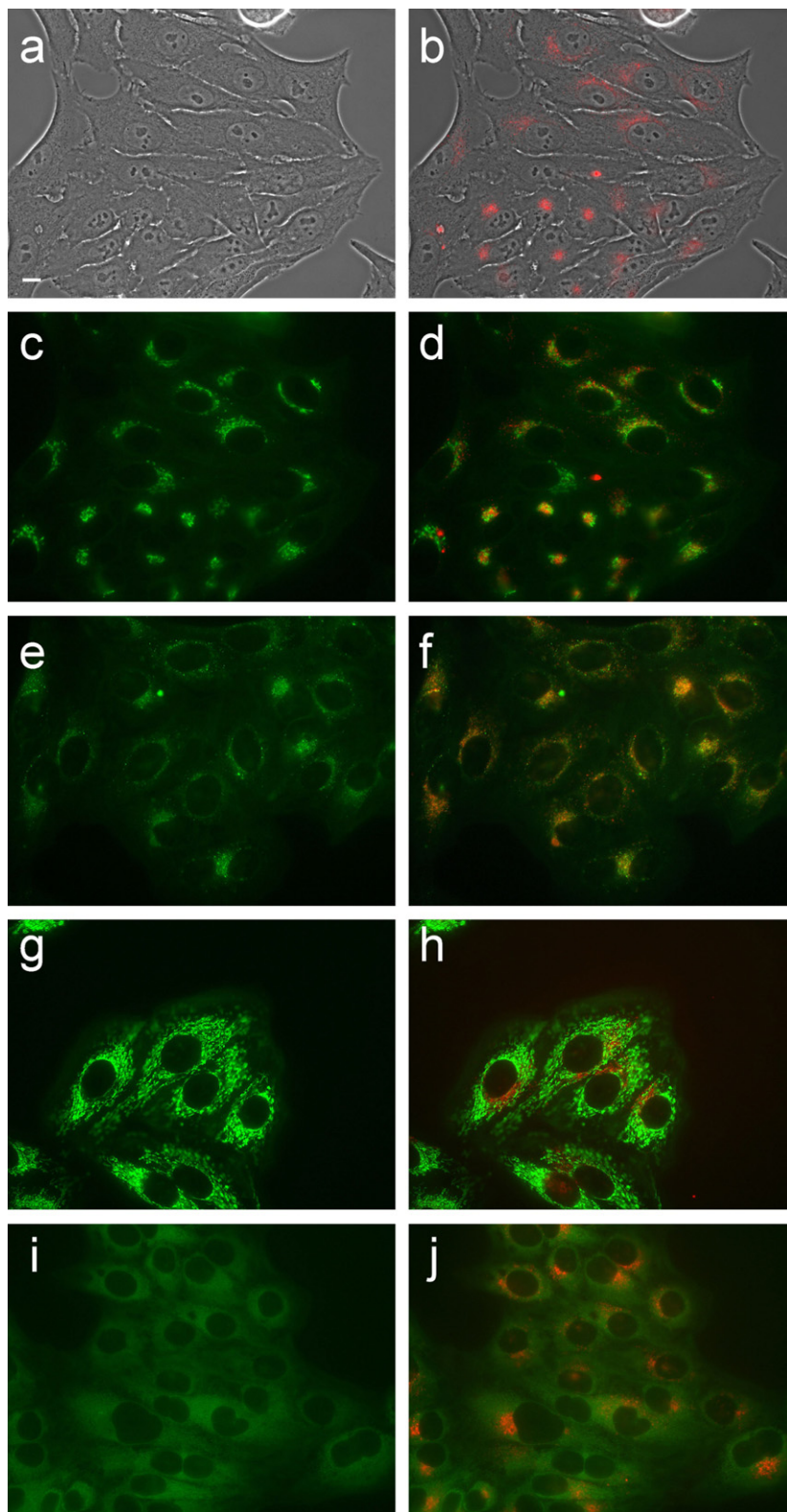
Figure 9. Intracellular localization of porphyrin **6c** in HEp2 cells at 10 µM for 24 h. (a) phase contrast; (b) porphyrin fluorescence; (c) BODIPY FL-C₅-Ceramide fluorescence (Golgi label); (d) overlay with porphyrin; (e) LysoSensor fluorescence (lysosome label); (f) overlay; (g) MitoTracker fluorescence (mitochondria label); (h) overlay; (i) ERTracker Green FM fluorescence (ER label); (j) overlay. Scale bar: 10 µm.

pyrrole (0.80 mL, 11.5 mmol) was purged with nitrogen for 5 min. TFA (2 µL, 0.023 mmol) was added and the final solution was stirred at room temperature in a sealed reaction vessel for 20 min. The light green crude material was dried onto silica and purified by silica gel column chromatography using methanol/dichloromethane 1:33. The title compound was obtained (65 mg) in 86% yield, as a yellow residue. [1]H
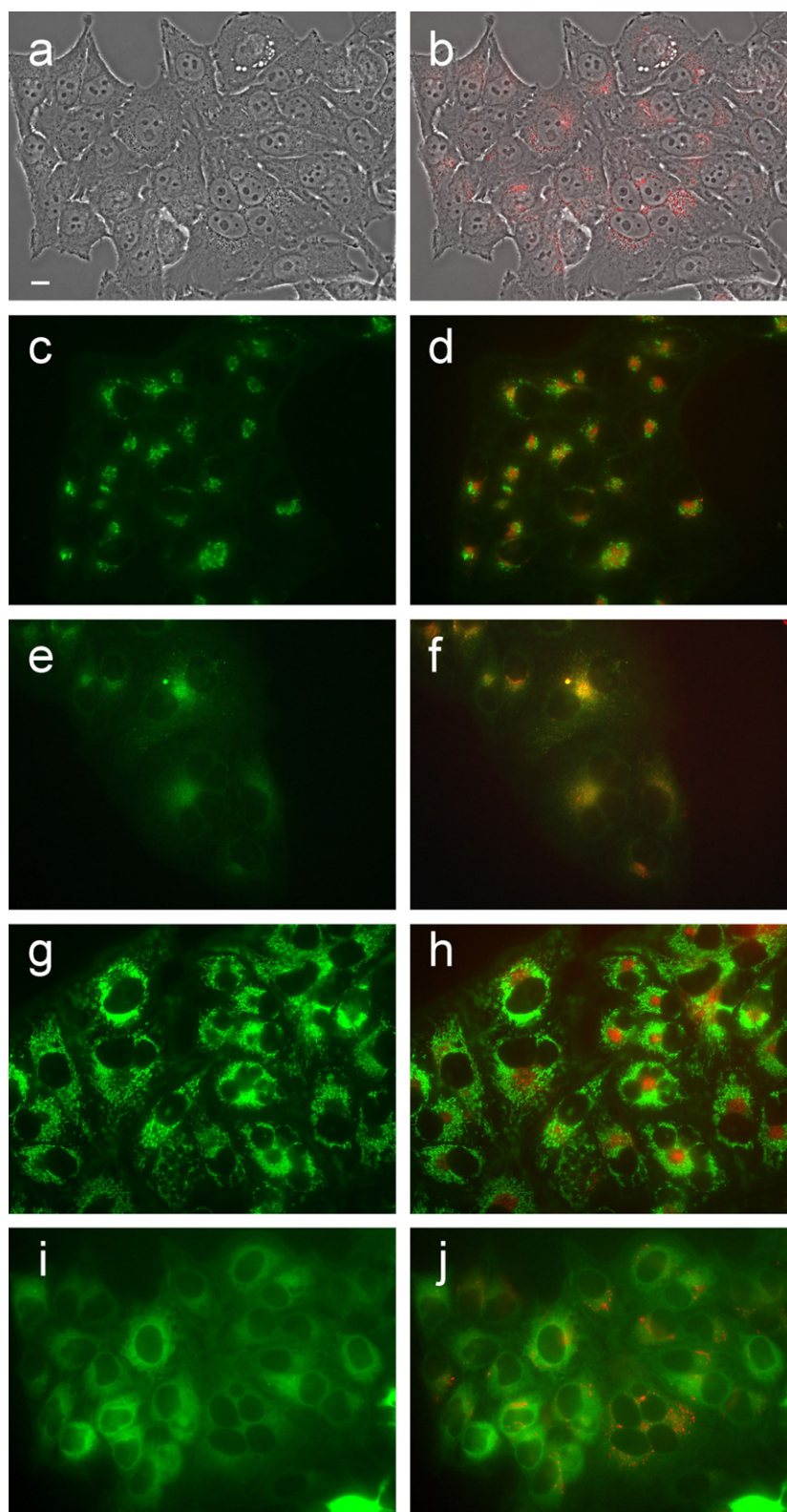
Figure 10. Intracellular localization of porphyrin **6d** in HEp2 cells at 10 µM for 24 h. (a) phase contrast; (b) porphyrin fluorescence; (c) BODIPY FL-C₅-Ceramide fluorescence (Golgi label); (d) overlay with porphyrin; (e) LysoSensor fluorescence (lysosome label); (f) overlay; (g) MitoTracker fluorescence (mitochondria label); (h) overlay; (i) ERTracker Green FM fluorescence (ER label); (j) overlay. Scale bar: 10 µm.

NMR (CDCl$_3$) δ ppm: 1.36 (t, 6H, CH$_3$, J = 7.0 Hz), 4.10 (m, 4H, CH$_2$), 5.60 (s, 1H, CH), 6.01 (s, 2H, o-ArH), 6.18 (s, 2H, m-ArH), 6.78 (s, 2H, α-H), 7.35 (m, 2H, β-H), 7.62 (m, 2H, β-H), 9.56 (br s, 2H, NH).

5.2. General procedure for porphyrin synthesis

A solution of dipyrromethane **4** (1.12 mmol) and bis[3,5-(2-methyl-o-carboran-1-yl)methyl]benzaldehyde **3**

Figure 11. Intracellular localization of porphyrin **7c** in HEp2 cells at 10 μM for 24 h. (a) phase contrast; (b) porphyrin fluorescence; (c) BODIPY FL-C$_5$-Ceramide fluorescence (Golgi label); (d) overlay with porphyrin; (e) LysoSensor fluorescence (lysosome label); (f) overlay; (g) MitoTracker fluorescence (mitochondria label); (h) overlay; (i) ERTracker Green FM fluorescence (ER label); (j) overlay. Scale bar: 10 μm.

(0.498 g, 1.12 mmol) in 112 mL of dichloromethane was purged with argon for 15 min. BF$_3$ · OEt$_2$ (0.283 mL, 2.23 mmol) was added and the reaction mixture was stir-

red in a sealed reaction vessel. After 1 h (for **4a**) or 4 min (for **4b**) DDQ (0.336 g, 1.48 mmol) and Et$_3$N (0.31 mL, 2.23 mmol) were added and the reaction mixture stirred
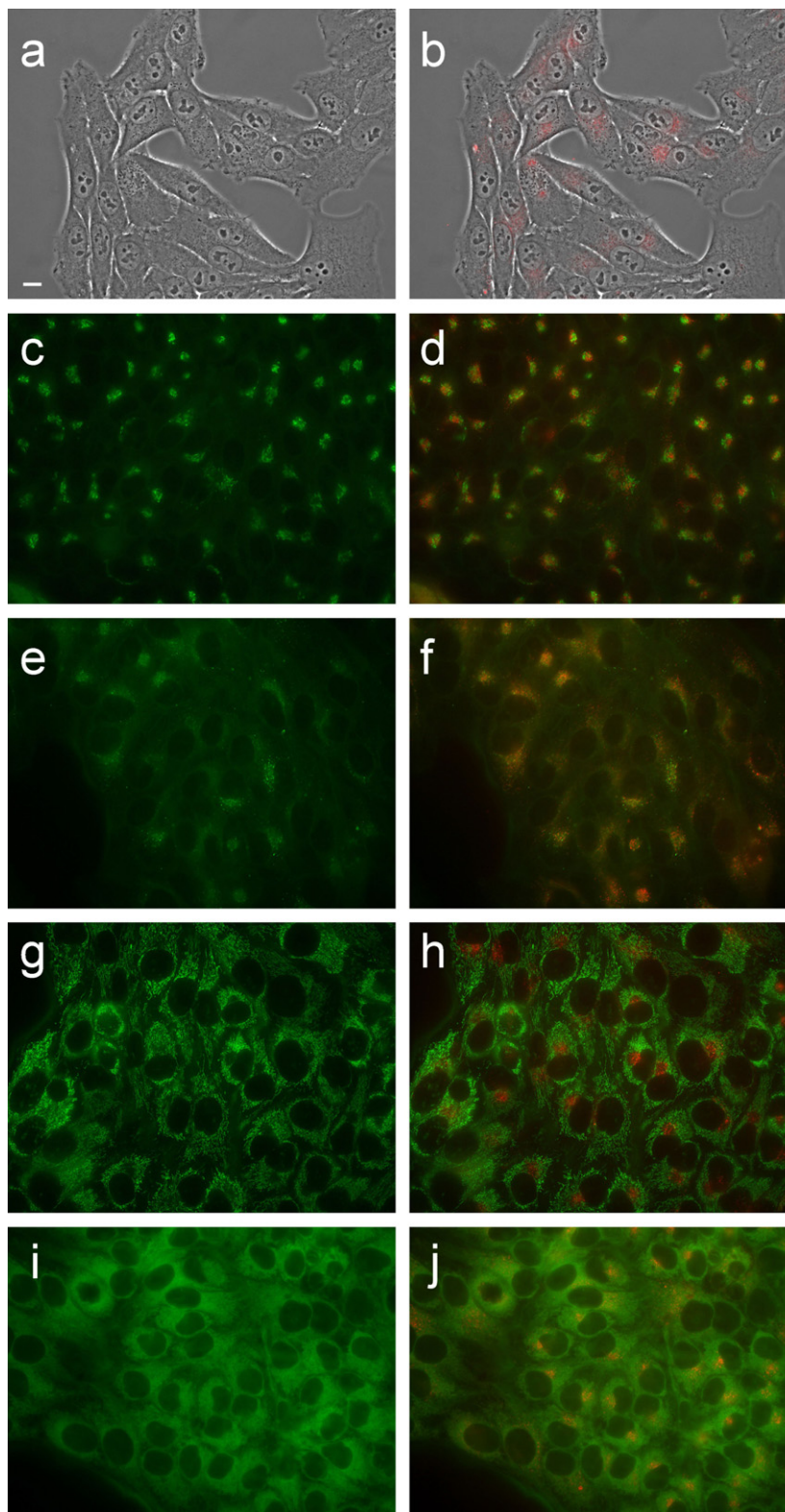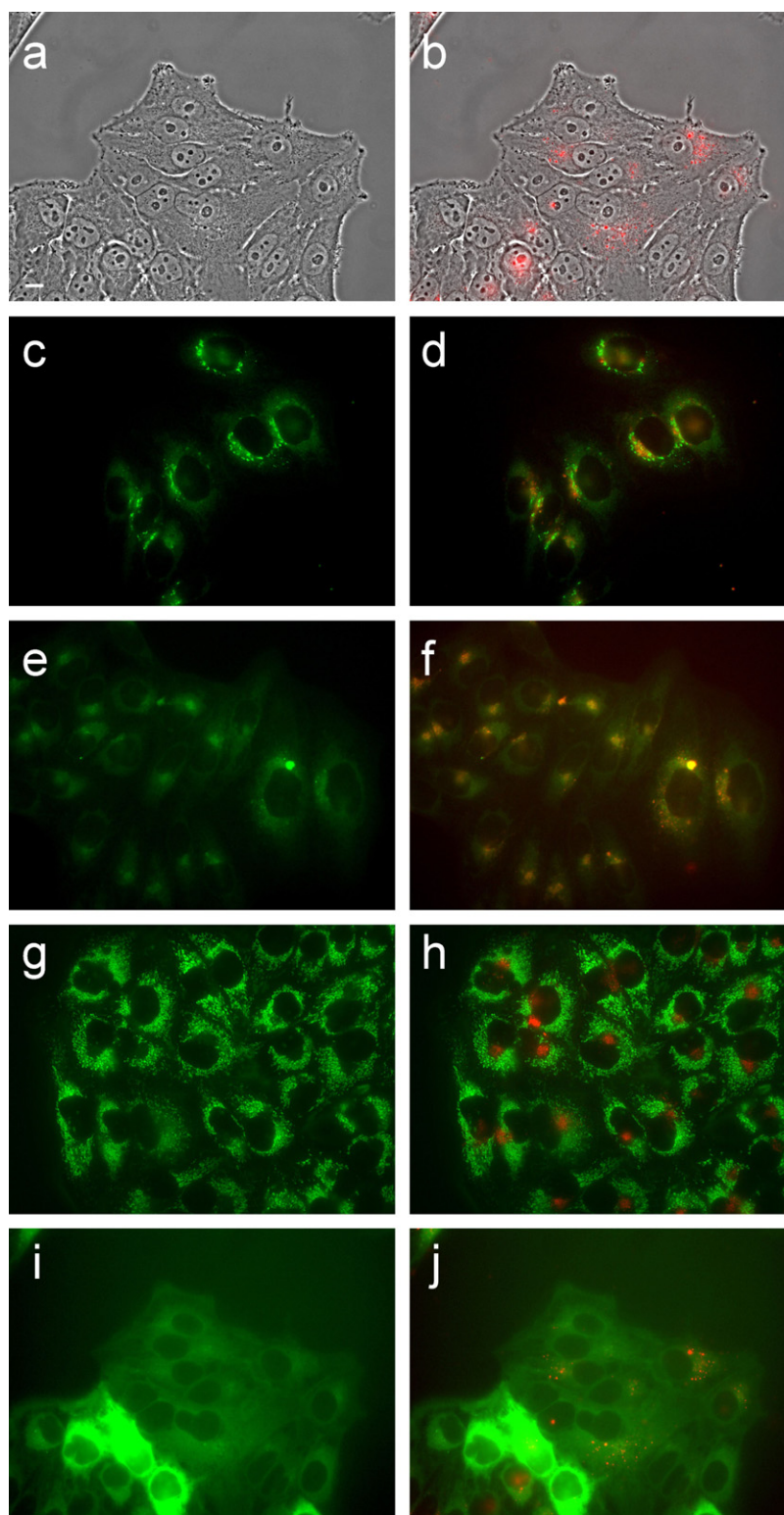
Figure 12. Intracellular localization of porphyrin **7d** in HEp2 cells at 10 μM for 24 h. (a) phase contrast; (b) porphyrin fluorescence; (c) BODIPY FL-C$_5$-Ceramide fluorescence (Golgi label); (d) overlay with porphyrin; (e) LysoSensor fluorescence (lysosome label); (f) overlay; (g) MitoTracker fluorescence (mitochondria label); (h) overlay; (i) ERTracker Green FM fluorescence (ER label); (j) overlay. Scale bar: 10 μm.

for 30 min. The mixture was then dried onto silica and filtered through a plug of silica gel using dichloromethane/hexane 2:1 for elution. The crude mixture was further purified using preparative silica TLC plates and dichloromethane/hexane 3:1 for elution to yield the porphyrins.

5.2.1. Deprotection. The diethyl ester porphyrins were dissolved in dichloromethane and purged with argon for 5 min. The reaction vessel was then sealed and bromotrimethylsilane was added by microliter syringe (16 equiv/phosphonate diester) while stirring at room temperature. The final mixture was stirred for 24 h.
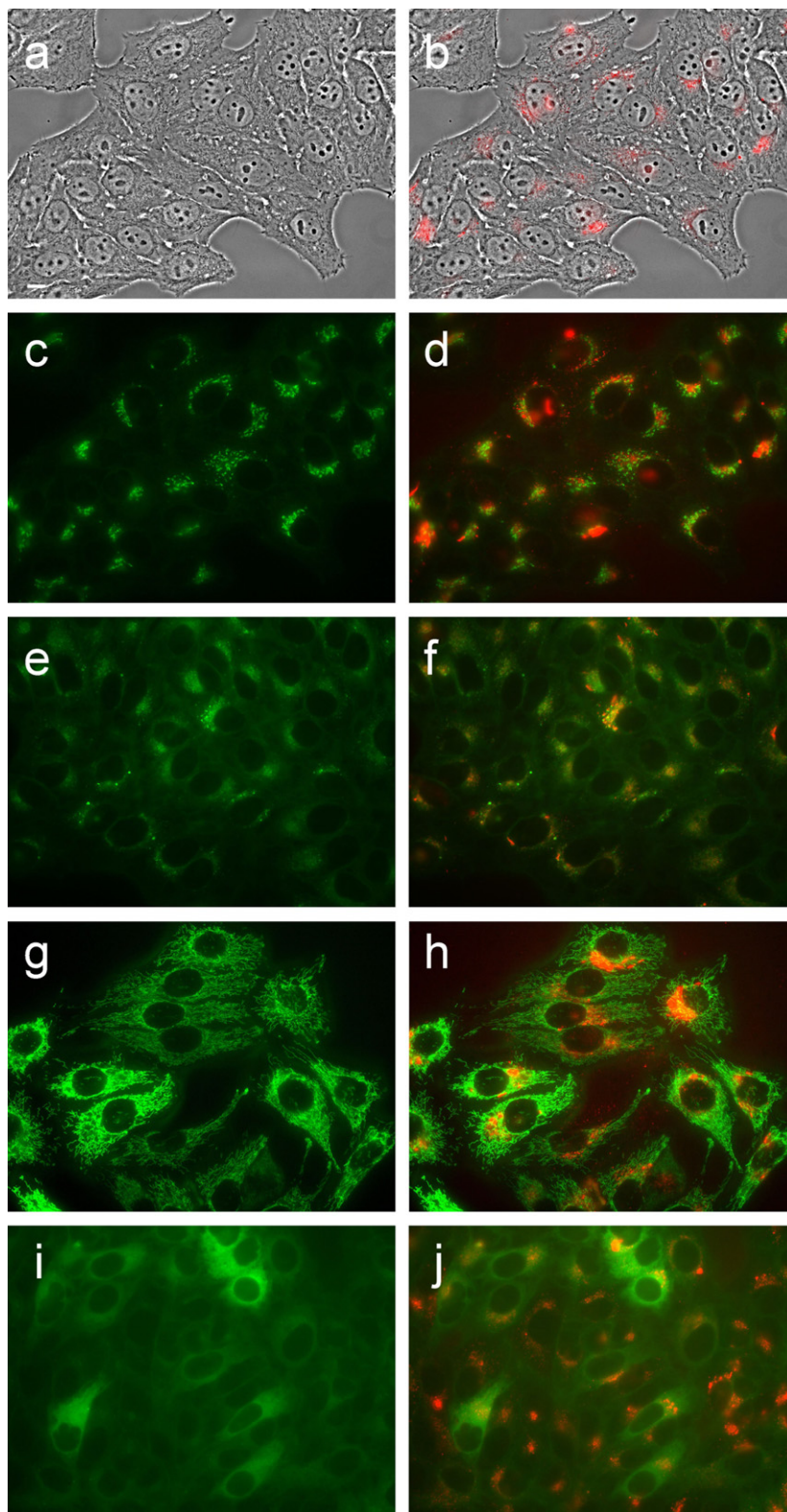
Figure 13. Intracellular localization of porphyrin **8d** in HEp2 cells at 10 μM for 24 h. (a) phase contrast; (b) porphyrin fluorescence; (c) BODIPY FL-C₅-Ceramide fluorescence (Golgi label); (d) overlay with porphyrin; (e) LysoSensor fluorescence (lysosome label); (f) overlay; (g) MitoTracker fluorescence (mitochondria label); (h) overlay; (i) ERTracker Green FM fluorescence (ER label); (j) overlay. Scale bar: 10 μm.

All solvents were removed under vacuum and the crude green residue was dissolved in a 1:4 H₂O/THF solution and allowed to stir for 2 h. The organic sol-

vent was removed under vacuum and the deprotected porphyrins were filtered and washed repeatedly with distilled water.

5.2.2. Quaternization. The dimethylamino porphyrins were dissolved in a 2:5 solution of CH_2Cl_2/CH_3I and the resulting mixture allowed to stand without stirring in a sealed reaction vessel for 72 h at room temperature. The quaternized products precipitated out of solution and were filtered and washed repeatedly with dichloromethane. Porphyrins **6c** and **7c** were partially demethylated upon standing over a period of one week (for **6c**) or one month (for **7c**), thus reforming the starting porphyrins **6a** and **7a**, respectively.

5.2.3. 5,15-Bis-(4-phosphonate diethyl ester)-10,20-bis[3,5-(2-methyl-*o*-carboran-1-yl)methylphenyl]porphyrin (5b). This porphyrin was obtained (31 mg, 3.6% yield) as a purple/red solid. Mp: >300 °C; MS (MALDI) *m/z* 1552.78 $[M-CH_3]^+$; ^{1}H NMR (CD_2Cl_2) δ ppm: −2.80 (br s, 2H, NH), 1.60 (t, 12H, CH_3, $J = 7.0$ Hz), 1.3–3.4 (br s, 40H, BH), 2.27 (s, 12H, CH_3), 3.85 (s, 8H, CH_2), 4.40 (m, 8H, CH_2), 7.58 (s, 2H, ArH), 8.12 (s, 4H, ArH), 8.26 (m, 4H, ArH), 8.40 (m, 4H, ArH), 8.95 (m, 8H, β-H). UV–Vis (CH_2Cl_2) λ_{max}: 419 nm (ε 331,000), 514 (15,400), 548 (6000), 588 (4800), 643 (2800). Deprotection afforded the corresponding phosphonic acid porphyrin (**5d**) in 83% yield as a green solid. Mp: >300 °C; HRMS (ESI) *m/z* 1457.0262 $[M+H]^+$, calculated for $C_{60}H_{88}B_{40}N_4O_6P_2$ 1456.0195; ^{1}H NMR (DMSO-d_6) δ ppm: −2.92 (br s, 2H, NH), 2.21 (s, 12H, CH_3), 1.3–3.4 (br s, 40H, BH), 3.92 (s, 8H, CH_2), 7.63 (s, 2H, ArH), 8.15 (br s, 8H, ArH), 8.29 (br s, 4H, ArH), 8.85 (br s, 8H, β-H). UV–Vis (DMSO) λ_{max}: 420 nm (ε 379,800), 515 (18,300), 550 (9100), 589 (6300), 645 (5300).

5.2.4. 5,10-Bis-(4-dimethylaminophenyl)-15,20-bis[3,5-(2-methyl-*o*-carboran-1-yl)methylphenyl]porphyrin (6a). This porphyrin was obtained in 2.1% yield as a black solid. Mp: >300 °C, MS (MALDI) *m/z* 1380.90 $[M^+]$; ^{1}H NMR (CD_2Cl_2) δ ppm: −2.69 (s, 2H, NH), 1.25–3.1 (br s, 40H, BH), 2.24 (s, 12H, CH_3), 3.25 (s, 12H, CH_3), 3.79 (s, 8H, CH_2), 7.17 (br s, 4H, ArH), 7.51 (s, 2H, ArH), 8.07–8.12 (m, 8H, ArH), 8.85 (br s, 4H, β-H), 8.99 (s, 2H, β-H), 9.03 (br s, 2H, β-H). UV–Vis (DMSO) λ_{max}: 423 nm (ε 171,000), 523 (13,500), 568 (14,200), 595 (8500), 657 (7300). Quaternization of this porphyrin afforded the corresponding quaternary ammonium iodide salt (**6c**) in 83% yield as a purple/red solid. Mp: >300 °C, HRMS (ESI) *m/z* 706.1089 $[M-2I]^{2+}$, calculated for $C_{66}H_{102}B_{40}N_6$ 706.1090; ^{1}H NMR (acetone-d_6) δ ppm: −2.79 (s, 2H, NH), 1.25–3.1 (br s, 40H, BH), 2.37 (s, 12H, CH_3), 4.07 (s, 8H, CH_2), 4.29 (s, 18H, CH_3), 7.86 (s, 2H, *p*-ArH), 8.22 (s, 4H, ArH), 8.55 (br s, 4H, ArH), 8.65 (br s, 4H, ArH), 8.88–8.99 (m, 8H, β-H). UV–Vis (DMSO) λ_{max}: 419 nm (ε 406,100), 514 (11,800), 548 (6300), 588 (4500), 644 (3200).

5.2.5. 5,10-Bis-(4-phosphonic acid diethyl ester)-15,20-bis[3,5-(2-methyl-*o*-carboran-1-yl)methylphenyl]porphyrin (6b). This porphyrin was obtained in 2.6% yield as a purple solid. Mp 282.8 °C; MS (MALDI) *m/z* 1552.78 $[M-CH_3]^+$; ^{1}H NMR (CD_2Cl_2) δ ppm: −2.83 (br s, 2H, NH), 1.55 (t, 12H, CH_3, $J = 7.0$ Hz), 1.3–3.4 (br s, 40H, BH), 2.27 (s, 12H, CH_3), 3.85 (s, 8H, CH_2), 4.39 (m, 8H, CH_2), 7.58 (s, 2H, ArH), 8.13 (s, 4H, ArH), 8.25 (m, 4H, ArH), 8.41 (m, 4H, ArH), 8.97 (m, 8H, β-H). UV–Vis (CH_2Cl_2) λ_{max}: 419 nm (ε 352,900), 514 (18,000), 549 (6800), 589 (5500), 643 (3400). Deprotection afforded the corresponding phosphonic acid porphyrin (**6d**) in 78% yield as a green solid. Mp >300 °C; HRMS (ESI) *m/z* 1457.0260 $[M+H]^+$, calculated for $C_{60}H_{88}B_{40}N_4O_6P_2$ 1456.0195; ^{1}H NMR (*d*-DMSO) δ ppm: −2.92 (br s, 2H, NH), 1.3–3.4 (br s, 40H, BH), 2.27 (s, 12H, CH_3), 3.97 (s, 8H, CH_2), 7.72 (s, 2H, ArH), 8.08–8.16 (br s, 8H, ArH), 8.32 (br s, 4H, ArH), 8.84 (m, 8H, β-H). UV–Vis (DMSO) λ_{max}: 419 nm (ε 395,100), 514 (17,200), 549 (8300), 589 (5900), 645 (4900).

5.2.6. 5-(4-Dimethylaminophenyl)-10,15,20-tris[3,5-(2-methyl-*o*-carboran-1-yl)methylphenyl] porphyrin (7a). This porphyrin was obtained in 6.3% yield as a red/brown solid. Mp >300 °C; MS (MALDI) *m/z* 1679.10 $[M]^+$; ^{1}H NMR (CD_2Cl_2) δ ppm: −2.73 (s, 2H, NH), 1.25–3.1 (br s, 60H, BH), 2.27 (s, 18H, CH_3), 3.29 (s, 6H, CH_3), 3.85 (s, 12H, CH_2), 7.20 (br s, 2H, ArH), 7.57 (s, 3H, ArH), 8.12–8.16 (m, 8H, ArH), 8.90 (br s, 6H, β-H), 9.10 (br s, 2H, β-H). UV–Vis (DMSO) λ_{max}: 418 nm (ε 253,900), 518 (14,300), 562 (11,000), 592 (8100), 653 (6300). Quaternization afforded the corresponding quaternary ammonium iodide salt (**7c**) in 92% yield as purple red solid. Mp 186.3 °C; HRMS (ESI) *m/z* 1695.7502 $[M+H-I]^+$, calculated for $C_{71}H_{122}B_{60}N_5$ 1694.5730; ^{1}H NMR (acetone-d_6) δ ppm: −2.78 (s, 2H, NH), 1.25–3.1 (br s, 60H, BH), 2.38 (s, 18H, CH_3), 4.09 (s, 12H, CH_2), 4.28 (s, 9H, CH_3), 7.85 (s, 3H, ArH), 8.23 (s, 6H, ArH), 8.60 (s, 4H, ArH), 8.92 (m, 8H, β-H); UV–Vis (DMSO) λ_{max}: 420 nm (ε 389,800), 514 (14,900), 548 (7700), 588 (5800), 644 (4400).

5.2.7. 5-(4-Phosphonic acid diethyl ester)-10,15,20-tris[3,5-(2-methyl-*o*-carboran-1-yl)methyl phenyl]porphyrin (7b). This porphyrin was obtained in 8.0% yield as a purple solid. Mp 294.7 °C; MS (MALDI) *m/z* 1756.10 $[M-CH_3]^+$; ^{1}H NMR (CD_2Cl_2) δ ppm: −2.80 (br s, 2H, NH), 1.36 (t, 6H, CH_3, $J = 7.0$ Hz), 1.3–3.4 (br s, 60H, BH), 2.28 (s, 18H, CH_3), 3.86 (s, 12H, CH_3), 4.38 (m, 4H, CH_2), 7.59 (s, 3H, ArH), 8.12 (s, 6H, ArH), 8.26 (m, 2H, ArH), 8.41 (m, 2H, ArH), 8.97 (m, 8H, β-H). UV–Vis (CH_2Cl_2) λ_{max}: 419 nm (ε 359,100), 514 (21,900), 548 (11,000), 588 (7400), 643 (3500). Deprotection afforded the corresponding phosphonic acid porphyrin (**7d**) in 94% yield as a black solid. Mp >300 °C; HRMS (ESI) *m/z* 1717.4781 $[M+H]^+$, calculated for $C_{68}H_{115}B_{60}N_4O_3P$ 1716.4735; ^{1}H NMR (DMSO-d_6) δ ppm: −2.91 (s, 2H, NH), 2.24 (s, 18H, CH_3), 1.3–3.4 (br s, 60H, BH), 3.92 (s, 12H, CH_2), 7.68 (br s, 3H, ArH), 8.12 (br s, 8H, ArH), 8.26 (br s, 2H, ArH), 8.86 (br s, 8H, β-H). UV–Vis (DMSO) λ_{max}: 420 nm (ε 418,100), 515 (16,900), 549 (8000), 589 (5700), 645 (4700).

5.2.8. 5,10,15-Tris-(4-phosphonic acid diethyl ester)-20-bis[3,5-(2-methyl-*o*-carboran-1-yl)methylphenyl]porphyrin (8b). This porphyrin was obtained in 4.5% yield as a purple solid. Mp 267 °C; MS (MALDI) *m/z* 1362.40

[M]$^+$; ^{1}H NMR (CD$_2$Cl$_2$) δ ppm: −2.83 (br s, 2H, NH), 1.55 (t, 18H, CH$_3$, J = 7.0 Hz), 1.3–3.4 (br s, 20H, BH), 2.27 (s, 6H, CH$_3$), 3.84 (s, 4H, CH$_2$), 4.40 (m, 12H, CH$_3$), 7.58 (s, 1H, ArH), 8.08 (s, 2H, ArH), 8.26 (m, 6H, ArH), 8.42 (m, 6H, ArH), 8.97 (m, 8H, β-H). UV–Vis (CH$_2$Cl$_2$) λ_{max}: 419 nm (ε 385,000), 514 (16,300), 549 (6700), 589 (5000), 643 (3000). Deprotection afforded the corresponding phosphonic acid porphyrin (**8d**) in quantitative yield as a blue-green solid. Mp: >300 °C; HRMS (ESI) *m/z* 1196.5739 [M+H]$^+$, calculated for C$_{52}$H$_{61}$B$_{20}$N$_4$O$_9$P$_3$ 1195.5655; ^{1}H NMR (DMSO) δ ppm: −2.94 (br s, 2H, NH), 1.3–3.4 (br s, 20H, BH), 2.27 (s, 6H, CH$_3$), 3.96 (br s, 4H, CH$_2$), 7.72 (s, 1H, ArH), 8.08–8.16 (m, 8H, ArH), 8.31–8.34 (m, 6H, ArH), 8.84 (br s, 8H, β-H). UV–Vis (DMSO) λ_{max}: 420 nm (ε 331,700), 515 (14,600), 549 (7100), 589 (5100), 645 (4200).

5.3. Molecular structures

Crystal structures were determined using data collected at low temperature on a Nonius KappaCCD diffractometer equipped with Mo Kα radiation (λ = 0.71073 Å) and a graphite monochromator. Refinement was by full-matrix least squares, and all nonhydrogen atoms were treated anisotropically with H atoms included, except as described below. Crystallographic data (excluding structure factors) for the structures in this paper have been deposited with the Cambridge Crystallographic Data Centre as supplementary publication nos. CCDC 663420–663423, CCDC 663925, and CCDC 644633. Copies of the data can be obtained, free of charge, on application to CCDC, 12 Union Road, Cambridge CB2 1EZ, UK (Fax: +44 (0)1223 336033 or e-mail: deposit@ccdc.cam.ac.uk).

Crystal data for **1**: colorless, C$_9$H$_7$Br$_2$N, M_r = 289.0, monoclinic space group $P2_1/c$, a = 7.574(2), b = 4.4039(10), c = 28.315(8) Å, β = 96.475(8)°, V = 938.4(4) Å^3, Z = 4, ρ_{calcd} = 2.045 g cm^{-3}, μ = 8.579 mm^{-1}, T = 90 K, 8408 data collected, R = 0.021 ($F^2 > 2\sigma$), R_w = 0.050 (all F^2) for 2279 unique data having θ < 28.2° and 110 refined parameters. Absorption corrections by multi-scan method.

Crystal data for **2**: colorless, C$_{15}$H$_{33}$B$_{20}$N, M_r = 443.6, monoclinic space group $P2_1/n$, a = 17.526(2), b = 7.8927(10), c = 20.262(3) Å, β = 109.743(6)°, V = 2638.0(6) Å^3, Z = 4, ρ_{calcd} = 1.117 g cm^{-3}, μ = 0.052 mm^{-1}, T = 150 K, 21359 data collected, R = 0.071 ($F^2 > 2\sigma$), R_w = 0.202 (all F^2) for 5089 unique data having θ < 27.1° and 328 refined parameters.

Crystal data for **3**: colorless, C$_{15}$H$_{34}$B$_{20}$O, M_r = 446.6, orthorhombic space group $P2_12_12_1$, a = 7.8923(10), b = 12.211(2), c = 27.548(5) Å, V = 2654.9(7) Å^3, Z = 4, ρ_{calcd} = 1.117 g cm^{-3}, μ = 0.054 mm^{-1}, T = 110 K, 22125 data collected, R = 0.050 ($F^2 > 2\sigma$), R_w = 0.143 (all F^2) for 4549 unique data having θ < 30.5° and 327 refined parameters.

Crystal data for **4a**: tan, C$_{17}$H$_{19}$N$_3$, M_r = 265.4, monoclinic space group $P2_1/n$, a = 8.0907(10), b = 8.735(2),

c = 20.075(4) Å, β = 96.093(12)°, V = 1410.7(5) Å^3, Z = 4, ρ_{calcd} = 1.249 g cm^{-3}, μ = 0.075 mm^{-1}, T = 110 K, 22814 data collected, R = 0.045 ($F^2 > 2\sigma$), R_w = 0.121 (all F^2) for 5080 unique data having θ < 32.5° and 189 refined parameters.

Crystal data for **5b**: brown, C$_{68}$H$_{104}$B$_{40}$N$_4$O$_6$P$_2$·3C$_7$H$_8$, M_r = 1844.3, monoclinic space group $C2/c$, a = 25.249(7), b = 22.017(6), c = 19.894(5) Å, β = 105.52(2)°, V = 10656(5) Å^3, Z = 4, ρ_{calcd} = 1.150 g cm^{-3}, μ = 0.092 mm^{-1}, T = 110 K, 48441 data collected, R = 0.112 ($F^2 > 2\sigma$), R_w = 0.343 (all F^2) for 7630 unique data having θ < 23.3° and 569 refined parameters. All toluene solvent molecules are disordered, and were treated in half-populated sites with isotropic C atoms and a common U_{iso} for each molecule. Solvent H atoms were not included.

Crystal data for **6a**: Black, C$_{64}$H$_{96}$B$_{40}$N$_6$·4CHCl$_3$, M_r = 1859.3, triclinic space group $P\bar{1}$, a = 11.3640(12), b = 18.753(2), c = 23.905(4) Å, α = 85.692(5), β = 86.915(5), γ = 73.912(6)°, V = 4878.1(11) Å^3, Z = 2, ρ_{calcd} = 1.266 g cm^{-3}, μ = 0.384 mm^{-1}, T = 106 K, 11914 data collected, R = 0.171 ($F^2 > 2\sigma$), R_w = 0.457 (all F^2) for 7736 unique data having θ < 20.0° and 573 refined parameters. Due to the very weak scattering power of the crystals even at low temperature, it was not possible to do full anisotropic refinement. Only the Cl atoms were refined anisotropically, while the lighter atoms were treated as isotropic.

5.4. Absorption and emission spectra

The absorption spectra were measured on a Perkin Elmer Lambda 35 UV–Vis spectrometer with 10 mm path length quartz cuvettes equipped with a photodiode detector, in the 300–700 nm wavelength range with 0.1 nm accuracy. Emission spectra were obtained on a Perkin Elmer LS55 luminescence spectrophotometer equipped with a Xenon lamp, in the 500–700 nm wavelength range with 1 nm accuracy. Stock solutions of all porphyrins in DMSO at 1×10^{-4} M were prepared. The aqueous solutions were prepared by adding 100 μL of each porphyrin DMSO stock solution into 10 mL of HEPES (N-2-hydroxyethylpiperazine-N′-2-ethanesulfonic acid) buffer, 20 mM, pH 7.4. All measurements were performed within 2 h of solution preparation.

5.5. Cell culture

HEp2 and T98G cells were acquired from the ATCC and maintained in a 50:50 mix of Advanced MEM:-DMEM supplemented with 5% FBS (all from Invitrogen). The cultures were passaged twice weekly to maintain subconfluent stocks. Each porphyrin was prepared as a 10 mM stock in DMSO and diluted to a working concentration of 10 μM in two stages. First, equal volumes of 10 mM stock and Cremophor EL (Fluka) were mixed in a microfuge tube and sonicated using a bath sonicator for 10 min. This mixture was then diluted with DMSO to a final porphyrin concentration of 1 mM. This was then diluted by dropwise addition

of medium to give a final concentration of 10 µM. The medium-containing porphyrin was then sonicated for 30 min.

5.5.1. Dark cytotoxicity. HEp2 cells were plated as described above and allowed 36–48 h to attach. The cells were then exposed to various concentrations of porphyrin up to 100 µM and incubated overnight. The loading medium was supplemented with CellTitre Blue (Promega) as per manufacturer's instructions. Cell viability was measured by reading the fluorescence at 520/584 nm using a BMG FLUOstar plate reader. The signal was normalized to 100% viable (untreated cells) and 0% viable (cells treated with 0.2% saponin (Sigma)).

5.5.2. Time-dependent cellular uptake. T98G cells were plated at 20000 per well in a Costar 96-well plate and allowed to grow for 36 h. Porphyrin stocks were prepared as above to 2× stocks. The porphyrin was then diluted in medium to final working concentrations. The cells were exposed to 10 µM porphyrin for 0, 1, 2, 4, 8, and 24 h. The uptake was stopped by removing the loading medium and by washing the cells with PBS. The cells were solubilized by the addition of 100 µl of 0.25% Triton X-100 (Calbiochem) in PBS. To determine compound concentration, fluorescence emission was read at 410/650 nm (excitation/emission) using a BMG FLUOstar plate reader. The cell numbers were quantified using Cy-Quant reagent (Molecular Probes).

5.5.3. Intracellular localization. HEp2 cells were plated on LabTek II two chamber coverslips and incubated for 36 h. The cells were then exposed to 10 µM of each porphyrin for 24 h. For co-localization experiments using organelle tracers, cells were incubated concurrently with compound the following morning for 30 min with the following organelle tracers: Mitochondria: MitoTracker Green (Molecular Probes) 250 nM; Lysosomes: LysoSensor Green (Molecular Probes) 50 nM; Endoplasmic reticulum: ERTracker Green FM (Molecular Probes) 2 µg/ml (for 1 h); Golgi: BODIPY FL- C_5-Ceramide (Molecular Probes) 1 mM. The slides were washed three times with growth medium and fed medium containing 50 mM HEPES, pH 7.4. Fluorescence microscopy was performed using a Zeiss Labovert 200 M inverted fluorescence microscope fitted with a standard FITC filter set (Ex/Em 470 nm/540 nm) for organelle tracers and standard Texas Red filter set (560 nm/600 nm LP) for compound detection (Chroma). The images were acquired with a Zeiss Axiocam MRM CCD camera fitted to the microscope.

Acknowledgment

Supplementary data

Dark cytotoxicity, fluorescence, and HRMS data for porphyrins are available. Supplementary data associated with this article can be found, in the online version, at doi:10.1016/j.bmc.2007.12.020.

References and notes

1. Barth, R. F.; Soloway, A. H.; Goodman, J. H.; Gahbauer, R. A.; Gupta, N.; Blue, T. E.; Yang, W.; Tjarks, W. *Neurosurgery* **1999**, *44*, 433–451.
2. Barth, R. F. *J. Neuro-Oncol.* **2003**, *62*, 1–5.
3. Barth, R. F.; Coderre, J. A.; Vicente, M. G. H.; Blue, T. E. *Clin. Cancer Res.* **2005**, *11*, 3987–4002.
4. Barth, R. F.; Joensuu, H. *Radiother. Oncol.* **2007**, *82*, 119–122.
5. Nakagawa, Y.; Pooh, K.; Kobayashi, T.; Kageji, T.; Uyama, S.; Matsumura, A.; Kumada, H. *J. Neuro-Oncol.* **2003**, *62*, 87–99.
6. Diaz, A. Z. *J. Neuro-Oncol.* **2003**, *62*, 101–109.
7. Busse, P. M.; Harling, O. K.; Palmer, M. R.; Kiger, W. S., III; Kaplan, J.; Kaplan, I.; Chuang, C. F.; Goorley, J. T.; Riley, K. J.; Newton, T. H.; Santa Cruz, G. A.; Lu, X.-Q.; Zamenhof, R. G. *J. Neuro-Oncol.* **2003**, *62*, 111–121.
8. Joensuu, H.; Kankaanranta, L.; Seppälä, T.; Auterinen, I.; Kallio, M.; Kulvik, M.; Laakso, J.; Vähätalo, J.; Kortesniemi, M.; Kotiluoto, P.; Serén, T.; Karila, J.; Brander, A.; Järviluoma, E.; Ryynänen, P.; Paetau, A.; Ruokonen, I.; Minn, H.; Tenhunen, M.; Jääskeläinen, J.; Färkkilä, M.; Savolainen, S. *J. Neuro-Oncol.* **2003**, *62*, 123–134.
9. Capala, J.; Stenstam, B. H.; Sköld, K.; af Rosenschöld, P. M.; Giusti, V.; Persson, C.; Wallin, E.; Brun, A.; Franzen, L.; Carlsson, J.; Salford, L.; Ceberg, C.; Persson, B.; Pellettieri, L.; Henriksson, R. *J. Neuro-Oncol.* **2003**, *62*, 135–144.
10. Soloway, A. H.; Tjarks, W.; Barnum, B. A.; Rong, F.-G.; Barth, R. F.; Codogni, I. M.; Wilson, J. G. *Chem. Rev.* **1998**, *98*, 1515–1562.
11. Bregadze, V. I.; Sivaev, I. B.; Glazun, S. A. *Curr. Med. Chem., Anti-Cancer Agents* **2006**, *6*, 75–109.
12. Renner, M. W.; Miura, M.; Easson, M. W.; Vicente, M. G. H. *Curr. Med. Chem., Anti-Cancer Agents* **2006**, *6*, 145–157.
13. Ratajski, M.; Osterloh, J.; Gabel, D. *Curr. Med. Chem., Anti-Cancer Agents* **2006**, *6*, 159–166.
14. Fairchild, R. G.; Bond, V. P. *Int. J. Rad. Oncol. Biol. Phys.* **1985**, *11*, 831–840.
15. Gabel, D.; Foster, S.; Fairchild, R. G. *Radiat. Res.* **1987**, *111*, 14–25.
16. This work was partially presented at the *12th International Congress on Neutron Capture Therapy for Cancer*, Takamatzu (Japan), October 2006: Vicente, M. G. H.; Easson, M. W. In *Proc. 12th ICNCT for Cancer*, 2006, pp 231–233.
17. Mettath, S.; Munson, B. R.; Pandey, R. K. *Bioconj. Chem.* **1999**, *10*, 94–102.
18. Bustamante, C.; Gurrieri, S.; Pasternack, R. F.; Purrello, R.; Rizzarelli, E. *Biopolymers* **1994**, *34*, 1099–1104.
19. Kessel, D.; Luguya, R.; Vicente, M. G. H. *Photochem. Photobiol.* **2003**, *78*, 431–435.
20. Sibrian-Vazquez, M.; Nesterova, I. V.; Jensen, T. J.; Vicente, M. G. H. *Bioconj. Chem.*, accepted for publication.
21. Gottumukkala, V.; Luguya, R.; Fronczek, F. R.; Vicente, M. G. H. *Bioorg. Med. Chem.* **2005**, *13*, 1633–1640.
22. Bodwell, G. J.; Bridson, J. N.; Houghton, T. J.; Yarlagadda, B. *Tetrahedron Lett.* **1997**, *38*, 7475–7478.
23. Vicente, M. G. H.; Wickramasinghe, A.; Nurco, D. J.; Wang, H. J. H.; Nawrocky, M. M.; Makar, M. S.; Miura, M. *Bioorg. Med. Chem.* **2003**, *11*, 3101–3108.

24. McIlroy, S. P.; Cló, E.; Nikolajsev, L.; Frederiksen, P. K.; Nielsen, C. B.; Mikkelsen, K. V.; Gothelf, K. V.; Ogilby, P. R. *J. Org. Chem.* **2005**, *70*, 1134–1146.

25. Lee, C.-H.; Lindsey, J. S. *Tetrahedron* **1994**, *50*, 11427–11440.

26. Littler, B. J.; Miller, M. A.; Hung, C.-H.; Wagner, R. W.; O'Shea, D. F.; Boyle, P. D.; Lindsey, J. S. *J. Org. Chem.* **1999**, *64*, 1391–1396.

27. Durantini, E. N. *Molecules* **2001**, *6*, 533–539.

28. Littler, B. J.; Ciringh, Y.; Lindsey, J. S. *J. Org. Chem.* **1999**, *64*, 2864–2872.

29. Smith, K. M.; Vicente, M. G. H.. In *Houben-Weyl Science of Synthesis*; Weinreb, S. M., Ed.; Georg Thieme: Stuttgart, 2004; Vol. 17, pp 1081–1235.

30. Muthukumaran, K.; Loewe, R. S.; Ambroise, A.; Tamaru, S.; Li, Q.; Mathur, G.; Bocian, D. F.; Misra, V.; Lindsey, J. S. *J. Org. Chem.* **2004**, *69*, 1444–1452.

31. Arsenault, G. P.; Bullock, E.; MacDonald, S. F. *J. Am. Chem. Soc.* **1960**, *82*, 4384–4389.

32. Senge, M. O.. In *The Porphyrin Handbook*; Kadish, K. M., Smith, K. M., Guilard, R., Eds.; Academic Press: San Diego, 2000; Vol. 1, pp 239–347.

33. Lauceri, R.; Purrello, R.; Shetty, S. J.; Vicente, M. G. H. *J. Am. Chem. Soc.* **2001**, *123*, 5835–5836.

34. Vicente, M. G. H.; Nurco, D. J.; Shetty, S. J.; Osterloh, J.; Ventre, E.; Hegde, V.; Deutsch, W. A. *J. Photochem. Photobiol. B: Biol.* **2002**, *68*, 123–132.

35. De Napoli, M.; Nardis, S.; Paolesse, R.; Vicente, M. G. H.; Lauceri, R.; Purrello, R. *J. Am. Chem. Soc.* **2004**, *126*, 5934–5935.

36. Hao, E.; Sibrian-Vazquez, M.; Serem, W.; Garno, J. C.; Fronczek, F. R.; Vicente, M. G. H. *Chem. Eur. J.* **2007**, *13*, 9035–9042.

37. Woodburn, K.; Phadke, A. S.; Morgan, A. R. *Bioorg. Med. Chem. Lett.* **1993**, *3*, 2017–2022.

38. Hill, J. S.; Kahl, S. B.; Stylli, S. S.; Nakamura, Y.; Koo, M.-S.; Kaye, A. H. *Proc. Natl. Acad. Sci. U.S.A.* **1995**, *92*, 12126–12130.

39. Vicente, M. G. H.; Edwards, B. F.; Shetty, S. J.; Hou, Y.; Boggan, J. E. *Bioorg. Med. Chem.* **2002**, *10*, 481–492.

40. Miura, M.; Micca, P. L.; Fisher, C. D.; Gordon, C. R.; Heinrichs, J. C.; Slatkin, D. N. *Br. J. Radiol.* **1998**, *71*, 773–781.

41. Ol'shevskaya, V. A.; Zaitsev, A. V.; Luzgina, V. N.; Kondratieva, T. T.; Ivanov, O. G.; Kononova, E. G.; Petrovskii, P. V.; Mironov, A. F.; Kalinin, V. N.; Hofmann, J.; Shtil, A. A. *Bioorg. Med. Chem.* **2006**, *14*, 109–120.

42. Ol'shevskaya, V. A.; Nikitina, R. G.; Zaitsev, A. V.; Luzgina, V. N.; Kononova, E. G.; Morozova, T. G.; Drozhzhina, V. V.; Ivanov, O. G.; Kaplan, M. A.; Kalinin, V. N.; Shtil, A. A. *Org. Biomol. Chem.* **2006**, *4*, 3815–3821.

43. Kubat, P.; Lang, K.; Cigler, P.; Kozisek, M.; Matejicek, P.; Janda, P.; Zelinger, Z.; Prochazka, K.; Kral, V. *J. Phys. Chem. B* **2007**, *111*, 4539–4546.

44. Matsumura, A.; Shibata, Y.; Yamamoto, T.; Yoshida, F.; Isobe, T.; Nakai, K.; Hayakawa, Y.; Kiriya, M.; Shimojo, N.; Ono, K.; Sakata, I.; Nakajima, S.; Okumura, M.; Nose, T. *Cancer Lett.* **1999**, *141*, 203–209.

45. Nguyen, T.; Brownell, G. L.; Holden, S. A.; Teicher, B. A. *Biochem. Pharma.* **1993**, *45*, 147–155.

46. Nguyen, T.; Brownell, G. L.; Holden, S. A.; Kahl, S.; Miura, M.; Teicher, B. A. *Radiat. Res.* **1993**, *133*, 33–40.

47. Callahan, D. E.; Forte, T. M.; Afzal, S. M. J.; Deen, D. F.; Kahl, S. B.; Bjornstad, K. A.; Bauer, W. F.; Blakely, E. A. *Int. J. Rad. Oncol. Biol. Phys.* **1999**, *45*, 761–771.

48. Hao, E.; Jensen, T. J.; Courtney, B. H.; Vicente, M. G. H. *Bioconj. Chem.* **2005**, *16*, 1495–1502.

49. Osterloh, J.; Vicente, M. G. H. *J. Porphyr. Phthalocya.* **2002**, *6*, 305–324.

50. Novick, S.; Laster, B.; Quastel, M. R. *Int. J. Biochem. Cell Biol.* **2006**, *38*, 1374–1381.